doi: 10.4302/plp.2011.3.09 PHOTONICS LETTERS OF POLAND, VOL. 3 (3), 116-118 (2011)

Analysis of the microstructured eutectic $Tb_3Sc_2Al_3O_{12}$-$TbScO_3$ photonic crystal properties

Agnieszka Mossakowska-Wyszyńska,[*1] Marcin Kaczkan,[1] Marcin Koba,[2,3]
Dorota Anna Pawlak,[4] Katarzyna Kołodziejak,[4] and Sebastian Turczyński[4]

[1]Institute of Microelectronics and Optoelectronics, Warsaw University of Technology, Koszykowa 75, 00-662 Warsaw, Poland
[2]Institute of Experimental Physics, University of Warsaw, Hoza 69, 00-681 Warsaw, Poland
[3]National Institute of Telecommunications, Szachowa1, 04-894 Warsaw, Poland
[4]Institute of Electronic Materials Technology, Wolczynska 133, 00-667 Warsaw, Poland

Received September 16, 2011; accepted September 28, 2011; published September 30, 2011

Abstract—In this paper, a numerical analysis of self-organized microstructured dielectric eutectic photonic crystal properties is presented. In particular, we study the terbium-scandium-aluminum garnet - terbium-scandium perovskite structure $Tb_3Sc_2Al_3O_{12}$-$TbScO_3$, grown by the micro-pulling down method. The self-organized dielectric microstructure is made of perovskite fibers embedded in a garnet phase matrix. In general, we analyzed the distribution of the electromagnetic field in the investigated periodic structures and the existence of a photonic band gap of such photonic crystals as a function of eutectic geometric parameters. Investigated structures do not reveal a wide photonic band gap, because of the low contrast of the refractive indices of individual phases.

In recent years, rapid development of theoretical and experimental research on photonic crystals [1] and metamterials [2] is observed. In the case of photonic crystals, when the wavelength of light is comparable with a period of the photonic crystal periodic structure, this structure exhibits a photonic band gap. In metamaterials, on the other hand, the wavelength should be much bigger than the structuring of the material since only the effective properties such as effective permittivity and permeability are important.

In this paper, we present an analysis of photonic properties of dielectric eutectic $Tb_3Sc_2Al_3O_{12}$-$TbScO_3$ (TSAG-TSP) terbium-scandium-aluminum garnet - terbium-scandium perovskite. The investigated structure, presented in Fig. 1, was obtained by self-organization during growth by the micro-pulling down method [3]. The eutectic is characterized by the formation of two unmixable crystals from a completely mixable melt. The most interesting eutectic structures, from the photonic crystals point of view, would be the microstructures with regular shapes, i.e., lamellar and rodlike shapes. To show how photonic properties change with eutectic geometric parameters, we analyze TSAG-TSP samples with three different pulling rates. The diameter of the microrods decreases with increasing the pulling rate [4].

[*] E-mail: A.Mossakowska@elka.pw.edu.pl

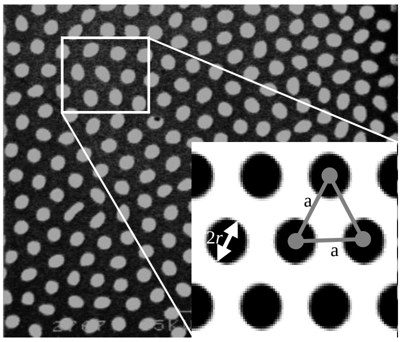

Fig. 1. SEM picture of self-organized pseudo-hexagonally packed TSAG-TSP eutectic microstructure: cross-section (the perovskite phase is gray and the garnet phase is black). The Structure is modelled by perfect hexagonal lattice with dimensions *r*- radius and *a*- period.

All the geometric parameters for each eutectic were calculated from SEM micrographs and then average parameters were obtained. These average parameters are shown in Table 1 for three different samples (Sample no.), where p.r. is the crystal pulling rate, 2*r* is the rod diameter in two perpendicular directions (hor.-horizontal, ver.-vertical, and aver.-averaged value), *a* is the period - average distance between rods, and *r/a* is the normalized ratio of average rod radius and crystal period. The investigated structure was modelled by perfect hexagonal lattice described by average rod radius *r* and crystal period *a*.

Table 1. Eutectic geometric parameters calculated from micrographs for three samples. Abbreviations are explained in main text.

Sample no.	p.r. [mm/min]	2*r* [μm]			*a* [μm]	*r/a*
		ver.	hor.	aver.		
1	0.15	3.08	3.56	3.14	4.81	0.33
2	0.45	1.74	1.74	1.74	2.90	0.30
3	1.00	1.21	1.28	1.18	2.41	0.24

In order to increase the contrast of the eutectic crystals refractive index, the investigated structures have been subjected to selective chemical etching. In this process, one eutectic phase was removed and therefore we investigated two new structures: first type $Tb_3Sc_2Al_3O_{12}$-air (TSAG-air), and second type air-$TbScO_3$ (air-TSP). Due to technological limitations, such microstructures were obtained with a height/depth of rod/hole of about 1μm, and were located on eutectic TSAG-TSP [3].

To perform numerical analysis of self-organized microstructure eutectic, we use refractive indices obtained by using a spectroscopic ellipsometer UVISEL, Horiba Jobin-Yvon in the range from 0.6 to 6.5eV (190-2100nm), and Bruker FTIR spectrometer in the spectral range 7500-550cm^{-1} [5]. Optical functions were obtained by fitting the data with a model dielectric function fulfilling the Kramers-Kronig dispersion relations [5].

To find the optical properties of self-organized eutectic microstructures, we used free software (MIT Photonic-Bands, MPB) with implemented Plane Wave Expansion Method PWEM [6, 7]. In addition, we assumed an infinite two-dimensional photonic structure with hexagonal lattice, which allowed us to use periodic boundary conditions. The rods and background material were homogenous in the perpendicular direction. This method allowed us to determine photonic crystal dispersion characteristics and analyze the photonic properties of investigated structures.

During numerical analysis, we calculated dispersion characteristics for the following eutectic structures: TSAG-TSP, TSAG-air and air-TSP of the three samples mentioned in Table 1. We made a series of numerical simulations which showed what should be the minimum of the refractive index of one eutectic phase for a constant refractive index of the second eutectic phase to have a photonic band gap of the investigated structure. We drew a lot of characteristics for different waveguide indices and a wide range of wavelengths for two kind of modes TE and TM.

All interesting results are summarized in Tables 2-4, where parameters for dispersion characteristics are shown. In Tables 2-4 we put: numerical calculation test number indicated in Tables column one as No.; three kinds of eutectic structures: TSAG-TSP, TSAG-air, air-TSP; refraction indices n_1 for eutectic warp and n_2 for eutectic rods, photonic bad gap PBG in percent calculated from frequency relation $[2(f_{max}-f_{min})/(f_{max}+f_{min})]\cdot 100\%$, the kind of mode and the wavelength range for the existing photonic band gap. Each numerical calculation test was performed for different eutectic structure and different refraction indices as indicated in Tables 2-4.

As we can see in Tables 2-4, photonic band gaps occur rather for TM mode and are very narrow, because the percent value of PBG is very low. All numerical simulations have some precision. In the used PWEM method, the obtained results of PBG at a level of 1% are on the border of error [6, 7]. Therefore we can say that in self-organized dielectric microstructure $Tb_3Sc_2Al_3O_{12}$-$TbScO_3$ it is very hard to observe a photonic band gap. It is so because this eutectic structure has too low contrast of the refractive indices of individual phases. Moreover, our analysis shows, that the investigated structures does not reveal a photonic band gap simultaneously for TE and TM modes for the same range of frequency and for all values of *k* vector. Samples, in which one of individual phases is replaced with air, have a photonic band gap inside a wavelength range of 4-8μm. The size of a photonic band gap is associated with an average distance between the rod cores and the crystal pulling rate. In the case of an eutectic structure having a photonic band gap, for the warp made of phase $Tb_3Sc_2Al_3O_{12}$, the minimum of core refractive indices should be between value 3 and 3.6. The spectral range for such a photonic band gap is located between 5.7-7.8μm, and it depends on the geometry of an eutectic structure.

Table 2. Simulation results for sample 1 (Sample No. 1 Table 1) for different numerical calculations (test No.) for different eutectic structures, and for different refractive indices.

No.	Structure	n_1	n_2	PBG [%]	Mode	λ range [μm]
1	TSAG-TSP	1.94	1.79	lack	-	-
2	TSAG-TSP	1.79	1.94	lack	-	-
3	TSAG-air	1.79	1.00	lack	-	-
4	TSAG-air	1.94	1.00	lack	-	-
5	air-TSP	1.00	1.79	0.91	TM	5.350-5.400
6	air-TSP	1.00	1.94	3.02	TM	5.410-5.580
7	air-TSP	1.00	1.935	2.95	TM	5.414-5.576
8	TSAG-TSP	1.94	3.49	1.04	TM	7.450-7.540
9	TSAG-TSP	1.84	3.49	2.47	TM	7.317-7.501
10	TSAG-TSP	1.84	3.30	1.01	TM	7.257-7.331
11	TSAG-TSP	1.79	3.22	1.04	TM	7.170-7.240
12	TSAG-TSP	1.68	3.22	2.72	TM	7.006-7.199
13	TSAG-TSP	1.68	3.02	1.04	TM	6.940-7.012

Table 3. Simulation results for sample 2 (Sample No. 2 Table 1) for different numerical calculations (test No.) for different eutectic structures, and for different refractive indices.

No.	Structure	n_1	n_2	PBG [%]	Mode	λ range [μm]
1	TSAG-TSP	1.94	1.79	lack	-	-
2	TSAG-TSP	1.79	1.94	lack	-	-
3	TSAG-air	1.79	1.00	1.50	TE	5.447-5.625
4	TSAG-air	1.94	1.00	0.51	TE	5.712-5.741
5	air-TSP	1.00	1.94	2.33	TM	5.566-5.697
6	air-TSP	1.00	1.79	0.38	TM	5.472-5.492
7	TSAG-TSP	1.82	3.56	1.06	TM	7.672-7.754
8	TSAG-TSP	1.69	3.28	1.02	TM	7.360-7.436

Table 4. Simulation results for sample 3 (Sample No. 3 Table 1) for different numerical calculations (test No.) for different eutectic structures, and for different refractive indices.

No.	Structure	n_1	n_2	PBG [%]	Mode	λ range [μm]
1	TSAG-TSP	1.94	1.79	lack	-	-
2	TSAG-TSP	1.79	1.94	lack	-	-
3	TSAG-air	1.79	1.00	lack	-	-
4	TSAG-air	1.94	1.00	lack	-	-
5	air-TSP	1.00	1.94	1.93	TM	4.32-4.40
6	air-TSP	1.00	1.97	2.35	TM	4.32-4.43
7	air-TSP	1.00	1.79	lack	-	-
8	TSAG-TSP	1.94	3.65	1.08	TM	6.00-6.06

9	TSAG-TSP	1.91	3.65	1.51	TM	5.96-6.05
10	TSAG-TSP	1.91	3.59	1.05	TM	5.95-6.02
11	TSAG-TSP	1.79	3.37	1.10	TM	5.76-5.82
12	TSAG-TSP	1.77	3.37	1.41	TM	5.74-5.82
13	TSAG-TSP	1.77	3.33	1.08	TM	5.73-5.79

Because of the limited volume of this paper, we show only three characteristics for investigated samples (as indicated in Table 1). In Figs. 2-4 we show dispersion characteristics for TM and TE modes. All Figures are plotted as a function of reciprocal lattice vector *k*. On the vertical axis is the normalized frequency expressed as dependence of ($\omega a/2\pi c$), where ω is the frequency and c is the velocity of light in free space.

In Fig. 2 we show the dispersion characteristics for eutectic structure sample 1 (Sample No. 1 Table 1) TSAG-TSP test 2 (No.2 Table 2), for which refraction indices are n_1=1.79 for eutectic warp and n_2=1.94 for eutectic rods. As we can see, the dispersion characteristics for two modes TE and TM overlap and for all normalized frequency the wave equation has a solution. Therefore, this eutectic structure has no photonic band gap.

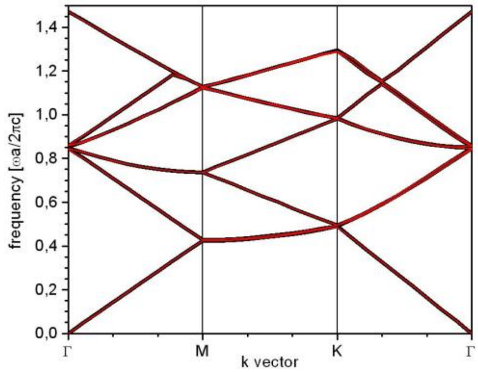

Fig. 2. Dispersion characteristic of structure TSAG-TSP sample 1 (Sample No. 1 Table 1) mode TE (black) and TM (red), numerical calculation test 2 (No.2 Table 2).

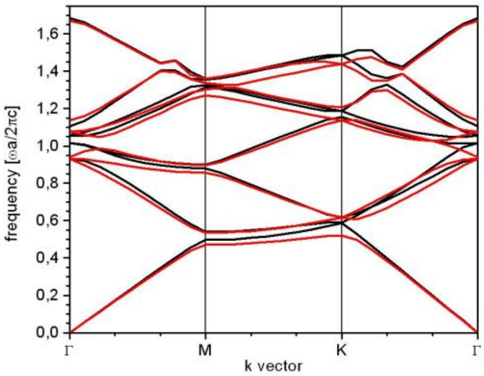

Fig. 3. Dispersion characteristic of structure air-TSP sample 1 (Sample No. 1 Table 1) mode TE (black) and TM (red), numerical calculation test 6 (No.6 Table 2).

Figure 3 shows the dispersion characteristics for eutectic structure sample 1 (Sample No. 1 Table 1) air-TSP test 6 (No.6 Table 2), for n_1=1.00, n_2=1.94. Here only for TM mode we observe the frequency ranges where the wave equation has no solution. That is why the mode cannot propagate in an eutectic structure and a photonic band gap appears. This photonic band gap is located between the first and the second bandwidth in a normalized frequency range from 0.526 to 0.538.

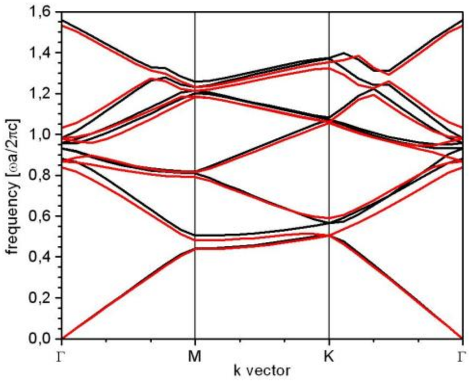

Fig. 4. Dispersion characteristic of structure TSAG-air sample 2 (Sample No. 2 Table 1) mode TE (black) and TM (red), numerical calculation test 3 (No.3 Table 3).

In Fig. 4 we show the dispersion characteristics for eutectic structure sample 2 (Sample No. 2 Table 1) TSAG-air test 3 (No.3 Table 3), for n_1=1.79, n_2=1.00. In contrast to Fig. 3, here a photonic band gap appears only for TE mode and is located between the first and second bandwidth in a normalized frequency range from 0.516 to 0.523. Similarly as in Fig. 3, a photonic band gap appears in particular M direction of the reciprocal lattice.

In conclusion, we have demonstrated numerical analysis of photonic properties of self-organized dielectric eutectic microstructures. In investigated structures it is very hard to observe a photonic band gap, because of too low contrast of the refractive indices of individual phases. Moreover, a microstructured eutectic does not reveal a photonic band gap simultaneously for TE and TM waveguide modes.

References

[1] E. Yablonowitch, Phys. Rev. Lett. **58**, 2059 (1987).

[2] J.B. Pendry, Phys. ReV. Lett. **85**, 3966 (2000).

[3] D.A. Pawlak, K. Kolodziejak, S. Turczynski, J. Kisielewski, K. Rozniatowski, R. Diduszko, M. Kaczakn, M. Malinowski, Chem. Matter. **18**, 2450 (2006).

[4] D.A. Pawlak, Scientia Plena **4**, 014801 (2008).

[5] K. Postava, L. Halagacka, D. Hrabovsky, O. Zivotsky, J. Pistora, D.A. Pawlak, S. Turczynski, K. Kolodziejak, Proc. SPIE **7353**, 735311 (2009).

[6] S.G. Johnson, J.D. Joannopoulos, The MIT Photonic-Bands Package, http://ab-initio.mit.edu/mpb/.

[7] S.G. Johnson, J.D. Joannopoulos, Opt. Exp. **8** 173 (2001), http://www.opticsinfobase.org/oe/abstract.cfm?URI=OPEX-8-3-173

